南華大學科技學院永續綠色科技碩士學位學程

碩士論文

Master Program of Green Technology for Sustainability
College of Science and Technology
Nanhua University

Master Thesis

崩塌地滲流侵蝕之臨界地下水位

Critical Groundwater Level of Landslide Dam due to Seepage Erosion

賴昕禾

Ratnadeep Sinha

指導教授：洪耀明 博士

Advisor: Yao-Ming Hong, Ph.D.

中華民國 110 年 7 月

July 2021

南 華 大 學

永續綠色科技碩士學位學程

碩 士 學 位 論 文

崩塌地滲流侵蝕之臨界地下水位

Critical Groundwater level of Landslide Dam due to Seepage Erosion

研究生：Ratnadeep Sinha
賴日斤未

經 考 試 合 格 特 此 證 明

口試委員：

李春元

張岩泰

洪耀明

指導教授：洪耀明

系主任(所長)：永續綠色科技碩士學位學程主任林文賜

口試日期：中華民國 110 年 7 月 2 日

Acknowledgments

At first, I would like to thank my thesis advisor, Professor Yao-Ming Hong, Associate Professor, Master Program of Green Technology for Sustainability, Nanhua University, Taiwan. The door to Professor Hong's office was always open whenever I ran into a trouble spot or had a question about my research or writing. He has always allowed this paper to be my work and steered me in the right direction whenever he thought I needed it.

中文摘要

自然土壩破壞的眾多破壞機制之一是滲流侵蝕引起的邊坡破壞。滲流侵蝕使土壤粘結鬆動，導致土壤結構失效。本研究通過實驗室試驗確定了滲流侵蝕引起的臨界地下水位。進行了砂箱實驗以模擬土壩與水的接觸。首先基於土壤的邊坡穩定性，發展破壞的臨界地下水位控制方程。其次以實驗室實驗，測試控制方程式之正確性。控制方程算出地下水的臨界高度為 19.117 厘米，實驗將地下水高度保持在 16 厘米、18 厘米和 20 厘米。試驗結果發現，大壩在地下水位達 18 厘米時發生潰壩，與方程式推算結果相近。

關鍵詞：滲流侵蝕，滑坡，滑坡壩，砂箱試驗，邊坡穩定

Abstract

One of the many failure mechanisms for natural earth dam failure is slope failure due to seepage erosion. Seepage erosion loosens the soil bonding causing failure in soil structure. This research determine the critical groundwater level due to seepage erosion by laboratory experiment. A sandbox experiment is done to recreate the landslide dam's exposure to water. A governing equation has been developed for the critical groundwater level for the failure of the landslide dam. The governing equation is based on the slope stability of the soil. Thereafter, that governing equation has been justified by the laboratory experiment. The experiment was done by varying the height of water near the value found by the governing equation. The governing equation gave the critical height of the groundwater is to be 19.117cm. the experiment was done keeping the heights of groundwater at 16cm, 18cm, and 20cm. The experimental result showed that the dam failed at an 18cm groundwater level. The result found by the experiment satisfies the value from the equation.

Keywords: seepage erosion, landslide, landslide dam, sandbox experiment, slope stability

Table of Content

List of Figure

List of Table

Chapter 1: Preface

1.1. Introduction

Landslide dams develop when a river is obstructed by mass movements such as rock avalanches, landslides, and debris flows caused by earthquakes, heavy rainfall, and other causes (Korup, 2002). Landslide dam failures may result in disastrous outburst floods (or debris flows) that inundate downstream regions, resulting in fatalities and property destruction (Evans, 1986; King et al., 1989; Walder & O'Connor, 1997; Becker et al., 2007). Landslide dams can vary in scale from a few cubic meters in volume and a few decimeters in height to multiple cubic kilometers in volume and several meters in height, and they can completely block an entire mountain valley (Hermanns, 2013). In all cases, the damming adds to the landslide hazard thanks to combinations of flooding of the valley upstream of the dam, diversion of the watercourse, and catastrophic flooding of downstream areas if the dam fails.

Natural dams can result in upstream flooding when the lake level increases and downstream flooding if the dam fails(Costa & Schuster, 1988). There are many examples of downstream flooding due to the failure of landslide dams, such as the Tsatichhu landslide dam in Bhutan, which failed due to dam-face saturation and progressive seepage (Dunning et al., 2006), Castle Lake near Mount St Helens, Washington, seepage-induced instabilities (Meyer et al., 1994), Bairaman landslide dam in Papua New Guinea, due to seepage (King et al., 1989).

Most landslide dams fail by overtopping (Costa & Schuster, 1988; Evans et al., 2011), when the landslide dammed lake fills with water, and erosion of the dam crest starts down cutting into the deposit. However, overtopping by displacement waves induced by a mass movement into a landslide-dammed lake has been confirmed and is a significant hazard where vast unstable slope

areas or glaciers occur above the lake (Hermanns et al., 2004). Other forms of breakdown include piping (Meyer et al., 1994), gradual upstream erosion (Hancox et al., 2005), and the downstream face of the dam slidingly collapsing (Beach et al., 2006). All of these processes are self-accelerating, as the more water that escapes growth, the faster the outflow velocity increases and the faster the material erodes. Consequently, erosion of landslide dams often results in breaching. Max discharges through such failures may be many times those of a river's seasonal peak flow, with amounts of many tens to more than 100,000 m3 /s (Evans et al., 2011). Such discharges have the potential to flood a considerable portion of the river valleys downstream, causing disruption and devastation to bridges, towns, farm fields, and hydropower infrastructure in the days following the wave's descent (Evans et al., 2011). These volumes of water and solids flushing downstream may significantly impact more than 1,000 km deep valleys (Schuster, 2006; Evans et al., 2011). This downstream sediment flush is not limited to the breach case itself but continues for years, causing aggravation in the river system (Davies & Korup, 2007). The failure of a landslide dam due to seepage erosion is the focus of this study. Seepage flow in a dam is defined as water movement from the dam's upstream to downstream sides via the embankment beneath the foundation base. Seepage in dams is primarily determined by soil properties such as plasticity, soil gradation, degree of compaction, and so on. Poorly graded soil has a lower resistance to seepage. The soil in the landslide dam is primarily poorly graded, and the degree of compaction is low due to self-compaction.

1.2. Structure of the study

This study consists of five chapters.

Chapter 1 is the preface, where the introduction and objective is discussed.

Chapter 2 is literature review, here the previous studies related this study is discussed.

Chapter 3 is theory and experiment, here all the theory related to the study is and the experiment procedure is discussed.

In chapter 4 the experimental outcome is discussed.

Chapter 5 is the conclusion, here the research is concluded.

1.3. Objective

The main objective of this study is to develop a governing equation for predicting the critical water level for landslide dam failure and create a small prototype of a landslide dam and expose it to the pore pressure to trigger the seepage erosion and critical velocity of the seepage erosion.

Chapter 2: Literature Review

2.1 Landslide Dam

In geologically active areas, landslide dams form mainly in steep and narrow valleys but also in open stream valleys. The most common landslide processes are the avalanches, slumps, slides, and flows caused by over-snow or precipitation, or earthquakes. At least six types of landslide dams vary morphologically, and the risk of failure and flooding varies accordingly (Costa & Schuster, 1988).

Table 2-1: Types of landslide dams according to their morphology

Types	Description
Type I	Dams are modest in comparison to the breadth of the valley floor and do not span the entire valley.
Type II	Dams are larger and span the valley floor, dropping debris high on opposite valley sides in some situations.
Type III	Dams fill the valley from side to side, travel long distances up and down the valley after the failure, and often involve the most landslide debris.
Type IV	Landslide dams are formed when material from both sides of a valley fails at the same time. The landslides can be next head-to-head in the valley's middle, or they can be juxtaposed.

Type V	Landslide dams form when a single landslide contains many lobes of debris that spread over the valley floor and construct two or more landslide dams in the same river reach.
Type VI	Landslide dams are made up of one or more failure surfaces that run beneath a stream or river valley and emerge on the other side of the valley from the landslide. Slow basal sliding and slumping are common features of these dams, which generate lakes by raising the height of the streambed and modifying the stream's local gradient.

Reference: (Costa & Schuster, 1988)

Landslide dams fail fast after training (half failed within ten days of formation, and only 15 percent last more than a year). The primary fault mechanism by far overtops and violates head-to-head erosion (Costa & Schuster, 1988). Milder slopes on the initial dam surface and higher gravel content in the dam will significantly strengthen the dam, reduce the likelihood of dam collapse, and thereby influence the flood. Cohesive clay can act to minimize seepage through the dam and subsequent subsidence, as well as significantly alter the timing and rate of the dam failure phase (Cao et al., 2011). The textural features of landslide dams, which are governed by particle size distribution and hydrodynamic conditions of the inflow discharge, have a significant impact on landslide dam collapse mechanisms and processes (Zhu et al., 2020).

A high steady water level in the reservoir or a progressive rise in the water level leads water to penetrate the dam body, increasing mobilized shear stress and causing the dam to break by rapid collapse when it gets larger than the dam's resistance to shear stress (Awal et al., 2007).

The rate at which the water level rises upstream of the dam body is determined by the rate of moisture migration within the dam. The saturated hydraulic conductivity and van Genuchten parameters, which are dependent on the sand mix and compaction, are the most important parameters for guiding moisture transport and, as a result, dam failure time (Regmi et al., 2013). The deformation behaviour of the landslide dam model is associated with the fluctuation in turbidity of the seepage flow. The hyper-concentrated seepage flow could be a sign that the landslide dam is about to fall. Turbidity can only be used for landslide dams with abundant fine particles during the early stages of internal erosion. Turbidity cannot be used in a landslide dam prone to long-term plumbing and internal erosion because the conveyed particle size may become too large to generate murky water (Wang et al., 2018).

Table 2-2: List of Landslide dams failed due to Seepage erosion.

Place	Type	Time to failure	Failure Mechanism	Reference
France Isere Department, NE of Livet Romanche River; St. Laurent Lake	Avalanche, rock /flow, debris	10,220 Days	Erosion of downstream face.	(Montandon, 1933); (Eisbacher, 1984)

India Uttar Pradesh State, Garwhal District Birehi Ganga River; Gohna Lake	Slide, rock	338 Days	Overtopping (with seepage)	(Holland, 1894);
Italy Calabria Region Buonamico River; Lake Costantino	Slide, rock /avalanche, rock	31 Days	Piping	(Guerricchio, 1973); (Ergenzinger, n.d.)
Peru Ayacucho Department, Cerro Condor-Seneca Mantaro River	Slide, rock	73 Days	Piping and seepage.	(Snow, 1964)
U.S.S.R. Kirghiz S.S.R., Kichik·Alay Mountains Tegermach River; Lake Yashilkul	Fall, rock and debris	48,000 Days	Piping	(Glazyrin & Reyzvikh, 1968); (Pushkarenko & Nikitin, 1988)

2.2 Seepage erosion of soil

The passage of a fluid, usually water, through the soil under a hydraulic gradient is known as seepage. If the 'hydraulic head' between the two places differs, a hydraulic gradient is anticipated to exist between them. The total of the location or datum head and the pressure head of water is referred to as the hydraulic head.

Seepage parallel to the path is the limited condition for a failure of the Coulomb type. Three factors: the fluctuation of the river phase, rise in the river phase, and the permeability of the soil control the number of sediment involved in the erosion of the sediment. The greater the range, the higher the river stage and the more permeable the active area of the inlet erosion. Cyclic aggravation and erosion of sediment are caused by the sediment contained by the stable slope of this drain and the maximum incline angle, depending on the regime of dam releases, local hydraulic conditions, and sediment availability. (Budhu & Gobin, 1995)

Increased porosity and reduced safety are given internal erosion is the result of migration of fines. For the stability of dams, the long-term density of fine particles is very important. The differences in porosity and the security factor between internal and non-erosion cases are small, where the long-term density of fine particles is almost identical to their initial density. In this situation, the incidence of inadvertent pitfall is the main factor. When analyzing the stability of natural dams, the internal erosion can be ignored to avoid complex calculations (Jiang et al., 2020).

When the seepage flow direction is perpendicular and emerging from the slope, it is the most critical condition for slope stability, and when the flow direction is vertically downward, it is the least critical (Ghiassian & Ghareh, 2008).

The maximum depth of erosion, rather than the volume of lost material, determines how much soil erosion contributes to the crucial Factor of Safety (Vandamme & Zou, 2013).

When the long-term density of tiny particles is nearly the same as the initial density, the difference in porosity and factor of safety between cases with and without internal erosion is minimal. As a result, seepage is the primary cause of slope failure (Jiang et al., 2020).

Coarse-grained soils and high infiltration rates result in the creation of positive pore water pressures, which cause the slope to collapse due to seepage forces. Fine-grained soils and low infiltration rates do not result in the creation of positive pore pressures, and failure occurs more frequently as a result of the loss of suction-induced shear power (Collins & Znidarcic, 2004).

2.3 Stability of Slope

Slope stability is commonly described in terms of shear stress and shear stress, with the majority of external factors increasing shear stress and the majority of internal factors decreasing shear strength (Terzaghi, 1962). Stability may be determined by examining the relationship between driving and resisting stresses. The production of shear stresses contributes to the collapse of the majority of landslide forms. The resisting stresses are the residue of reactionary stresses and can be thought of as the slope's mobilized shear power in relation to the shear stresses (McColl, 2015). The geometry of the slope, initial loading conditions, boundary conditions, and other material properties all play a role in slope stability analyses, as does the choice of appropriate shear strength values (Gündo, n.d.).

Slopes, both natural and man-made, are often categorized as finite or infinite. The equilibrium of force acting on a probable slope failure surface can be used to examine the stability of a finite slope. The complexity of a finite slope's stability analysis is determined by the nature of the materials the slope and the

loading circumstances associated with the probable failure surface. An infinite slope is a slope with a constant slope and a small depth. The soil is considered to be homogeneous in most circumstances, however, an infinite slope could contain non-homogeneous material (Ahmad, n.d.). There is a maximum stable seepage slope below which slope failures are uncommon for sandbars if instability is induced by outward groundwater seepage. Depending on the dam discharge regimes, sands deposited between this maximum stable seepage slope and the maximum depositional slope angle will cyclically aggravate and erode. For freshly deposited sediments subjected to externally directed seepage forces, the maximum stable seepage slope provides the desired failure surface (Budhu & Gobin, 1995).

Chapter 3: Theory and Methodology

3.1. Theory

3.1.1 Seepage

Seepage, also known as seepage flow, is the slow movement of liquid through small gaps or cracks in the surface of unsaturated soil in hydrology. Seepage flow weakens the soil mass. And seepage is one of the most common factors in the failure of earthen dams, whether it is natural or men made. It directly affects the stability of the dam slope due to a rise in the pore water pressure, which leads to internal erosion, which further leads to piping.

The phreatic line, the pore pressure inside the dam or in its base, the exit gradient at the dam's downstream face, and the amount of seepage flow that can pass through the dam's cross-sections are all investigated during the seepage analysis in the earth dam.

3.1.2 Effective stress

The relationship between water pressure and mobilized stress in a soil matrix is determined by effective stress. Simply put, it's known as:

$$\boldsymbol{\sigma'} = \boldsymbol{\sigma} - \mathbf{P_w} \qquad (1)$$

Effective Stress ($\boldsymbol{\sigma'}$) = Actual pressure of the soil

Total stress ($\boldsymbol{\sigma}$) = The total pressure of the soil.

Pore Water Pressure ($\boldsymbol{u}$) = The pore water pressure.

3.1.3 Slope stability

Slope stability is the primary means of quantitatively assessing the level of stability of a slope, done using a Factor of Safety. Soil tends to fail in shear; these concepts directly govern slope failures. Soil has shear strength, conventionally defined as friction and cohesion. • At a given shear surface, there is shear stress, induced by:

• The gravitational mass of the soil.

• Water pressures.

• Overloading, seismicity, etc.

Figure 1 shows the the gravity forces and seepage erosion acting on an element from a slope of infinite slope. The governing equation is derived as follows.

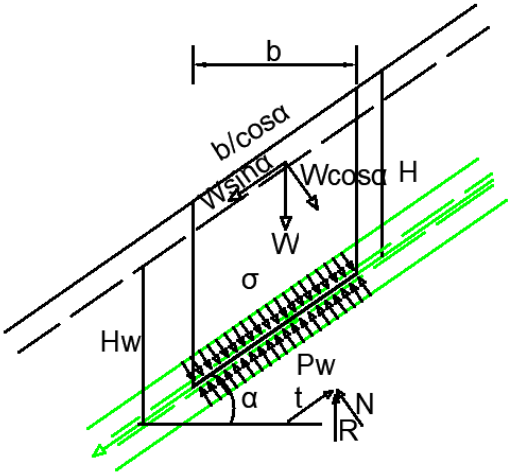

Figure 3-1: Infinite slope

Assuming that soil gravity and water gravity are the principal factors on changes in slope movement. The difference between destabilising forces (τ), which are based on weight and slope and are constant, and resisting forces (τ_r), which are based on water pressure at the slip surface, governs the landslide dynamics. The normal, lifting, and shear stresses can be defined as follows, assuming forces vertical and parallel to the slope (洪耀明, 2018):

$$\sigma = \frac{W\cos\alpha}{b/\cos\alpha} = \frac{\gamma bH\cos\alpha}{b/\cos\alpha} = \gamma H\cos^2\alpha \qquad (1)$$

and

$$p_w = \frac{\gamma_w H_w\cos\alpha}{b/\cos\alpha} = \gamma_w H_w\cos^2\alpha \qquad (2)$$

and

$$\tau = \frac{S}{b/\cos\alpha} = \frac{\gamma bH\sin\alpha}{b/\cos\alpha} = \gamma H\sin\alpha\cos\alpha \qquad (3)$$

Where α is the slope angle; γ is the specific weight of solid; H is the height from slip slope to the surface; Hw is the height from slip slope to the water table.

For a local point of the landslide where infinite slope conditions apply, resisting forces can be estimated using Mohr-Coulomb criterion, depending on cohesion and friction as follows:

$$\tau_r = c + (\sigma - p_w)tan\varphi = c + (\gamma H - \gamma_w H_w)\cos^2\alpha\tan\varphi \qquad (4)$$

where c is the cohesion, σ is the normal stress, p_w is the groundwater pressure, and φ is the friction angle, all magnitudes referred to the slip

surface (Corominas et al., 2005). p_w is the temporal variable in the resisting shear stress. The critical condition occurs in $\tau=\tau_r$. A large GL will increase p_w, and decrease τ_r, and induce landslide finally. Replacing Eq. (4), the threshold of groundwater level p_{wc} can be written as

$$P_{wc} = \sigma - (\tau - c)/\tan\varphi \quad (5)$$

Substituting P_{wc} by H_{wc} by Equcation (1b), the maximum groundwater level H_{wc} will be

$$H_{wc} = (\gamma/\gamma_w)\mathrm{H} - (\gamma H \sin\alpha\cos\alpha - c)/(\gamma_w \cos^2\alpha \tan\varphi) \quad (6)$$

Equation (6) displays that H_{wc} is the function of specific weight of solid and water, the resisting forces, the cohesion, the slope angle, and the frictionn angle.

3.2. Laboratory Experiments

3.2.1. Preliminary Experiments

Calibration is mostly used to ensure that the sensors (soil pressure and pore pressure meter) are compliant with our assumptions. The most effective method is to attain relationships by the use of laboratory instruments and resources with well-defined constitutive relationships. Real-world landslides cannot be used to calibrate models since the timing of real-world landslides is unclear, and the aspects of motion are not well understood. The experimental experiment was conducted in our laboratory using a setup called 'sandbox.' The setup allowed mass to move along a path as the pore water pressure in the sand mass increased, simulating the lateral spreading caused by internal stresses.

Calibration is used to equate those parameters derived from the simulations to the observed values. The criteria include the increase of pore water pressure inside the sand mass, the displacement of sand, and so on. For calibrating the sensors, initial measurements were taken, and a graph was plotted; the linear

equation was then determined from the graph. The following figure shows the pressure at different depths in the soil.

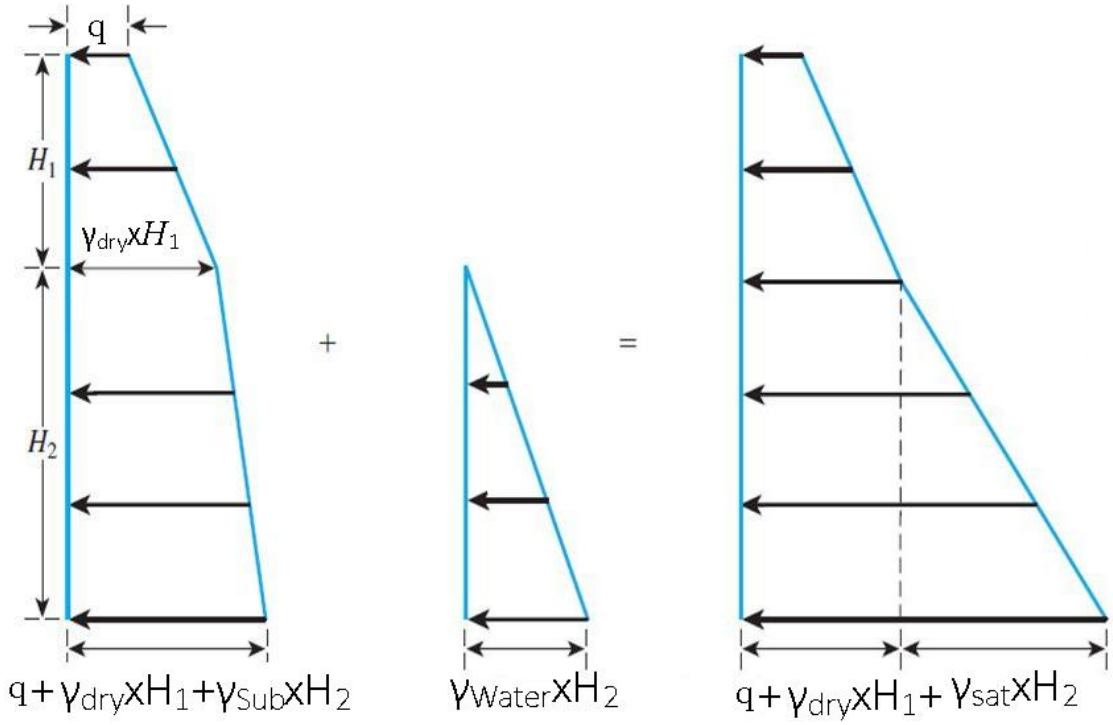

Figure 3-2: Effective Pressure, Pore Pressure and Total pressure at different depth

Soil sensor

The sensors are exposed to the soil load and their behaviour is recorded to formulate an equation according the characteristics they gave in the different loads.

Figure 3-3: Setup for calibration of soil sensor

Procedure:

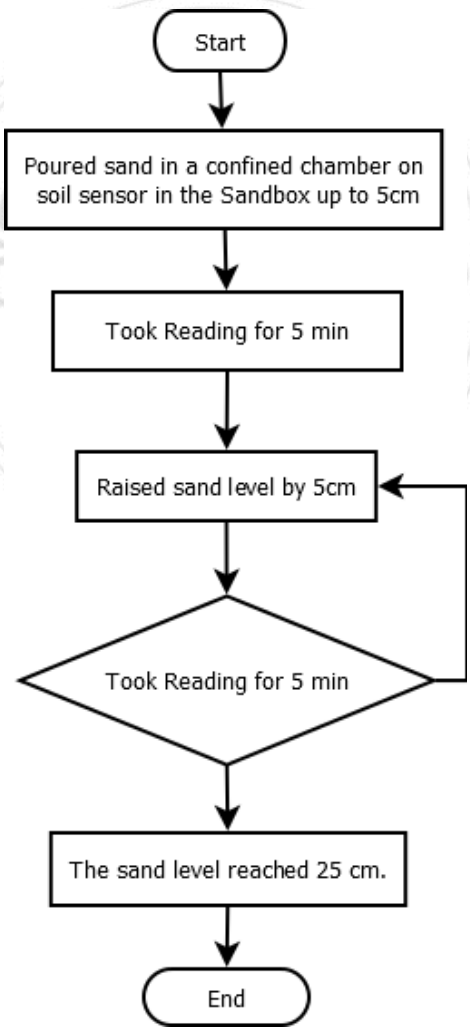

Sensor 1

Table 3-1: Soil Sensor 1 readings

Height of soil (cm)	Soil Transducer 1 (Mv)
5	3.218
10	3.224
15	3.222
20	3.225
25	3.226
30	3.225

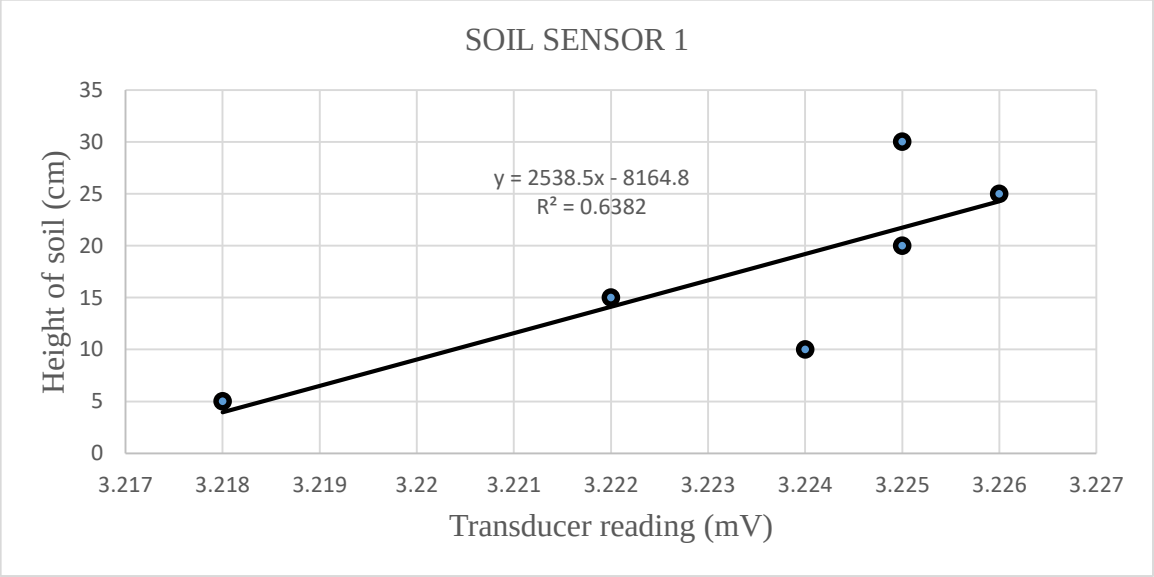

Figure 3-4: Graph for soil sensor 1 calibration

Sensor 2

Table 3-2: Soil Sensor 2 readings

Height of soil (cm)	Soil Transducer 2 (Mv)
5	4.123
10	4.126
15	4.129
20	4.132
25	4.135
30	4.137

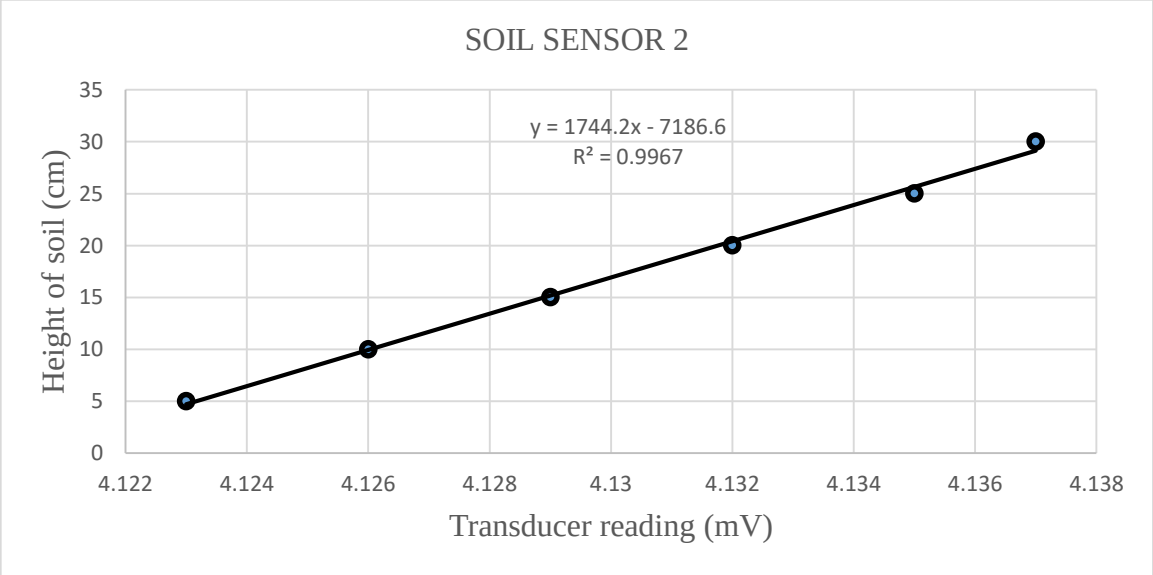

Figure 3-5: Graph for soil sensor 2 calibration

Sensor 3

Table 3-3: Soil Sensor 4 readings

Height of soil (cm)	Soil Transducer 3 (Mv)
5	3.255
10	3.261
15	3.263
20	3.266
25	3.267
30	3.267

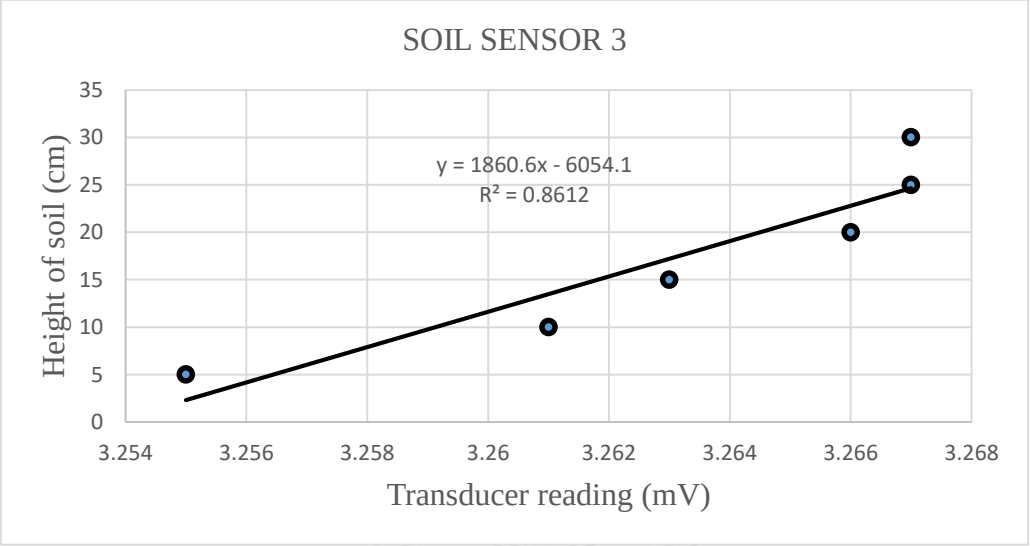

Figure 3-6: Graph for soil sensor 3 calibration

Sensor 4

Table 3-4: Soil Sensor 4 readings

Height of soil (cm)	Soil Transducer 4 (Mv)
5	3.941
10	3.95
15	3.957
20	3.963
25	3.968
30	3.97

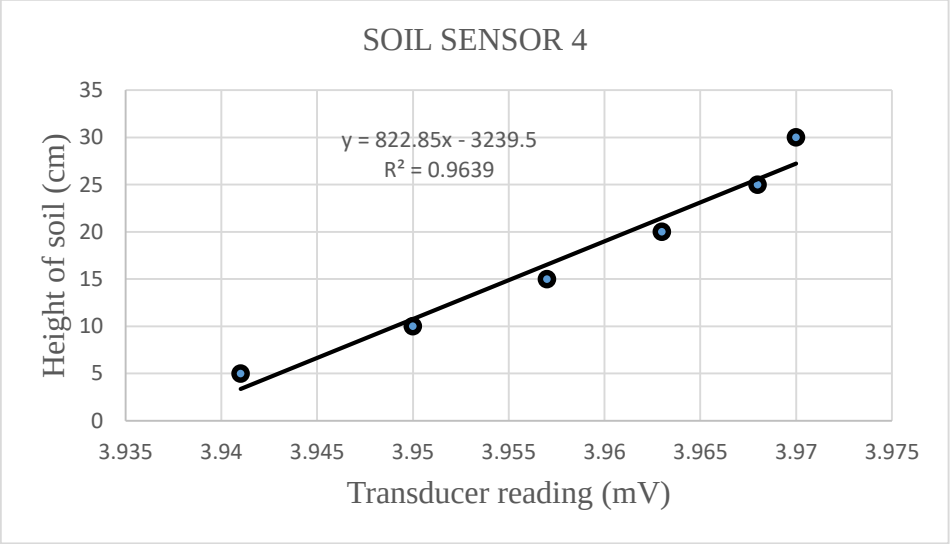

Figure 3-7: Graph for soil sensor 4 calibration

Pore pressure sensor

The sensors are exposed to the water load and their behaviour is recorded to formulate an equation according the characteristics they gave in the different loads.

Figure 3-8: Setup for calibration of soil sensor

Procedure:

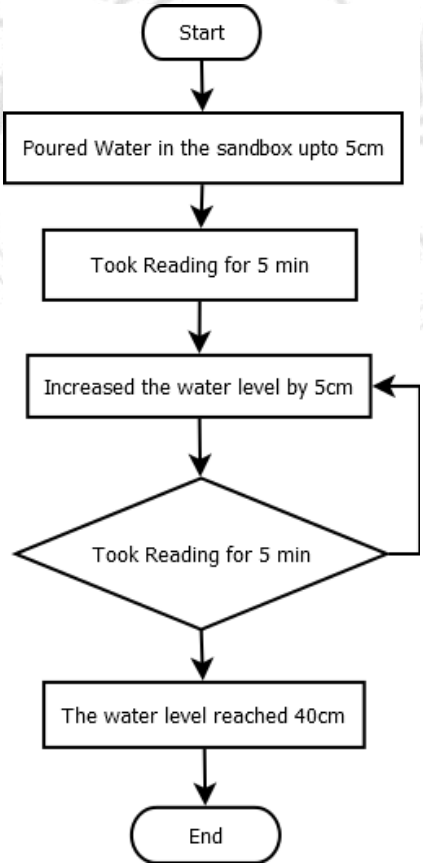

Sensor 1

Table 3-5: Water Sensor 1 readings

Sensor (mV)	Height of water(cm)	Pressure(KN/m^2)
0.071	0	0
0.08	5	0.4905
0.087	10	0.981
0.095	15	1.4715
0.103	20	1.962
0.111	25	2.4525
0.117	30	2.943
0.125	35	3.4335
0.133	40	3.924

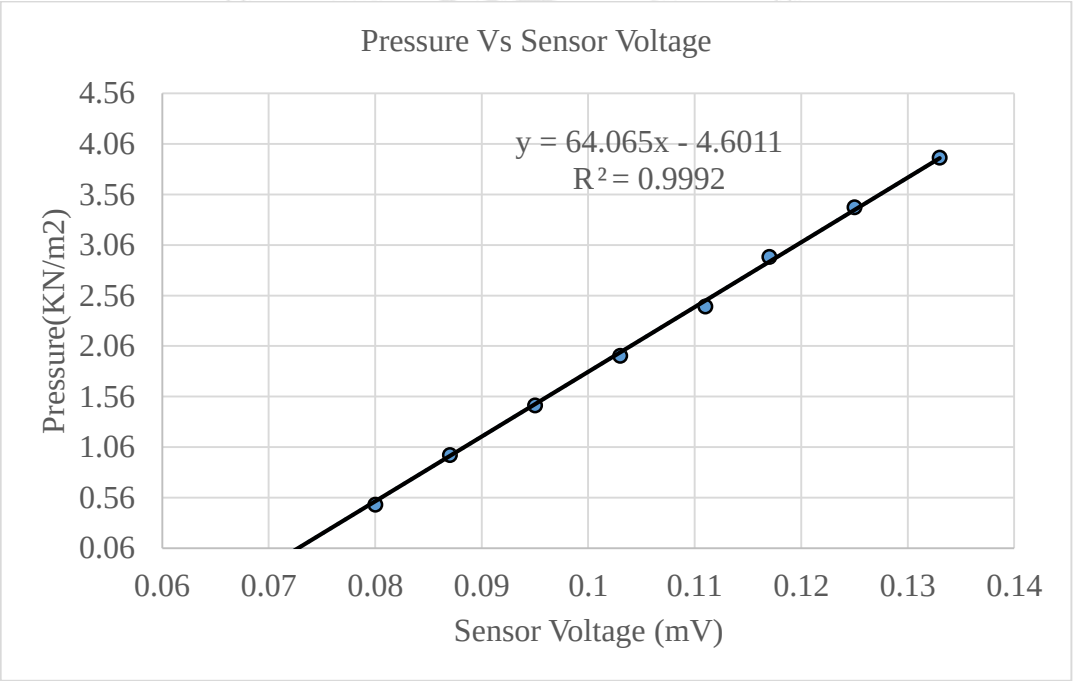

Figure 3-9: Graph for water sensor 1 calibration

Sensor 2

Table 3-6: Water Sensor 2 readings

Sensor (mV)	Height of water(cm)	Pressure(KN/m^2)
0.003	0	0
0.013	5	0.4905
0.018	10	0.981
0.027	15	1.4715
0.034	20	1.962
0.043	25	2.4525
0.05	30	2.943
0.058	35	3.4335
0.065	40	3.924

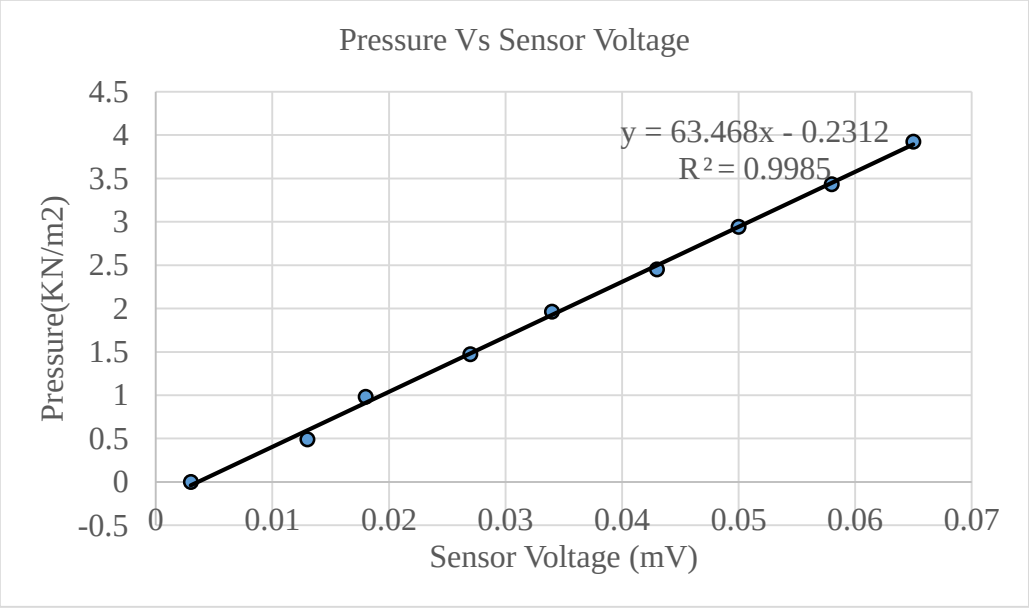

Figure 3-10: Graph for water sensor 2 calibration

Sensor 3

Table 3-7: Water Sensor 3 readings

Sensor (mV)	Height of water(cm)	Pressure(KN/m^2)
0.298	0	0
0.308	5	0.4905
0.314	10	0.981
0.325	15	1.4715
0.333	20	1.962
0.342	25	2.4525
0.349	30	2.943
0.358	35	3.4335
0.365	40	3.924

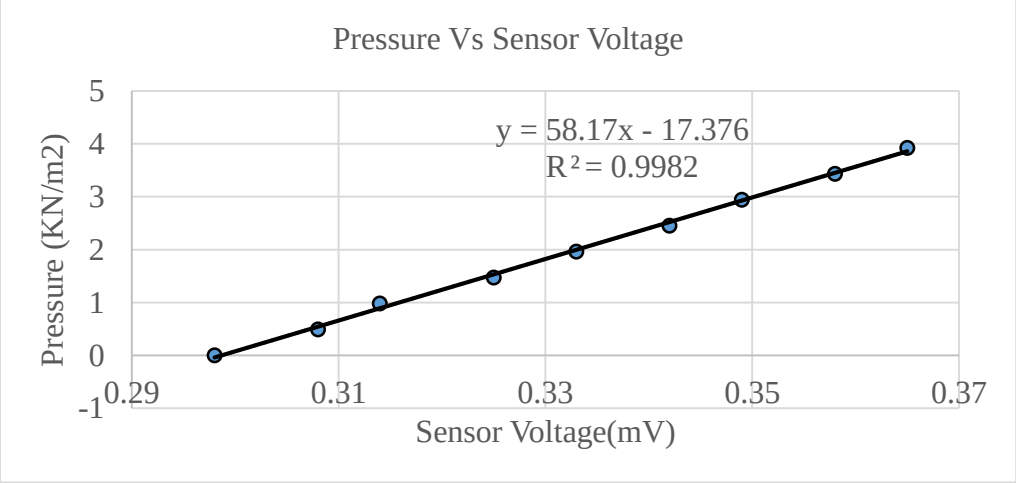

Figure 3-11: Graph for water sensor 3 calibration

Sensor 4

Table 3-8: Water Sensor 4 readings

Sensor (mV)	Height of water(cm)	Pressure(KN/m^2)
0.069	0	0
0.08	5	0.4905
0.091	10	0.981
0.102	15	1.4715
0.112	20	1.962
0.124	25	2.4525
0.133	30	2.943
0.144	35	3.4335
0.155	40	3.924

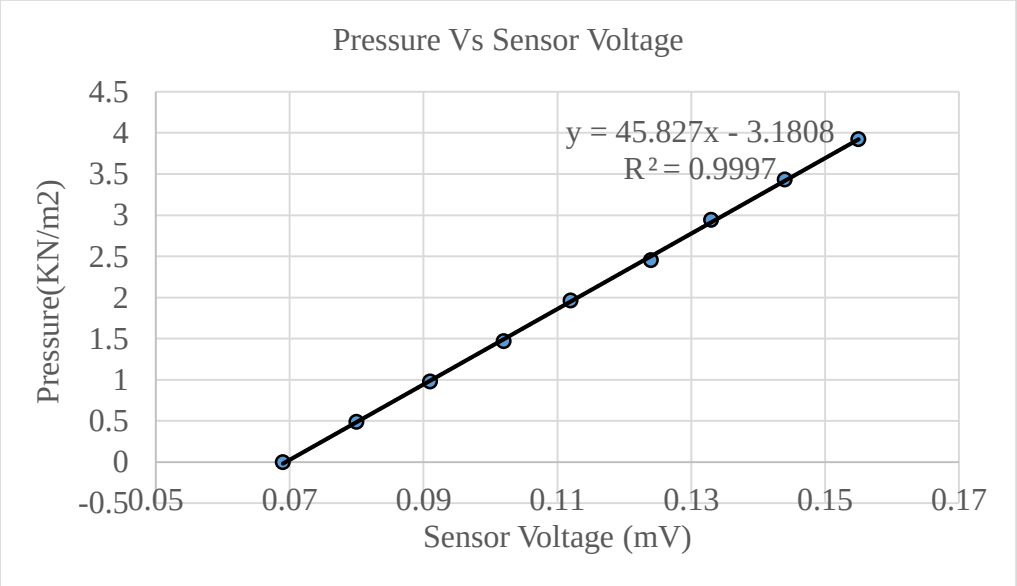

Figure 3-12: Graph for water sensor 4 calibration

Soil And Water Together
Procedure:

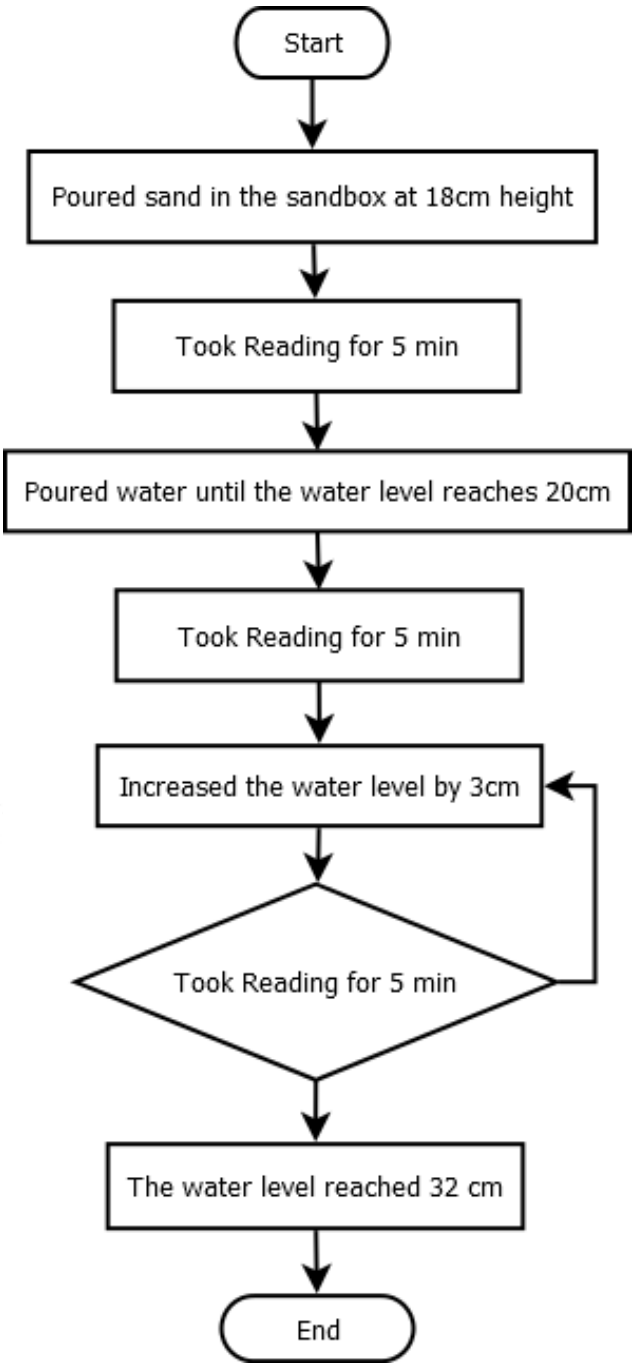

Figure 3-13: Setup for sensor calibration when subjected to water and soil both

Table 3-9: Transducer reading when subjected to sand and water both

Sl No	pore (CH1) mV	sand (CH1)	pore (CH2)	Sand (CH2)	Pore (CH3)	Sand (CH3)	Pore (CH4)	Sand (CH4)	Pore (CH0)	Sand (CH5)	Height
1	0.08	3.224	-0.007	4.119	0.295	3.285	0.084	3.146	-0.038	3.939	18
2	0.083	3.23	0.018	4.123	0.307	3.289	0.09	3.149	-0.038	3.942	20
3	0.087	3.233	0.025	4.127	0.312	3.29	0.094	3.149	-0.038	3.946	23
4	0.09	3.235	0.028	4.13	0.316	3.291	0.101	3.15	-0.038	3.949	26
5	0.095	3.237	0.033	4.133	0.324	3.292	0.108	3.152	-0.038	3.952	29
6	0.1	3.239	0.037	4.134	0.328	3.293	0.115	3.154	-0.038	3.955	32

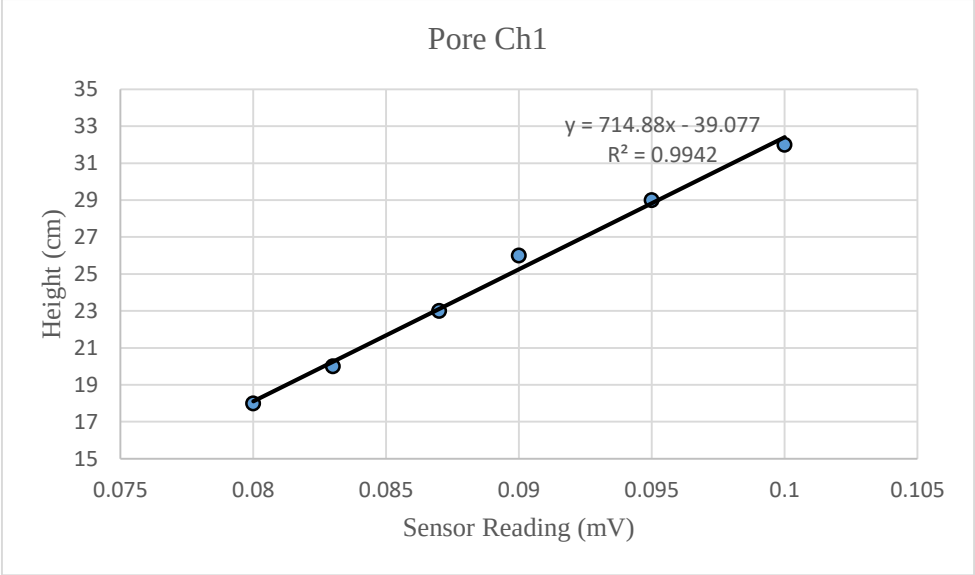

Figure 3-14: Graph for water sensor 1 when subjected to sand and water

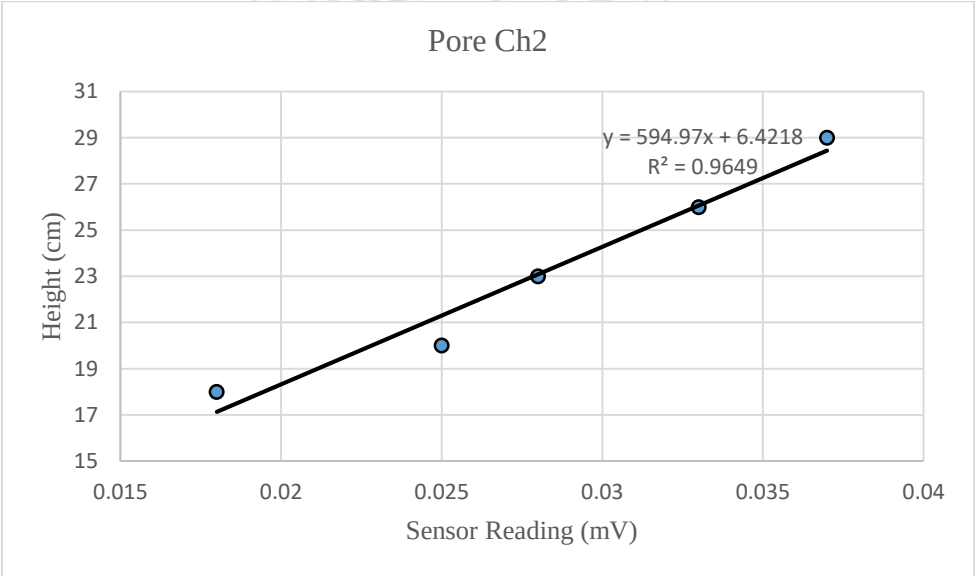

Figure 3-15: Graph for water sensor 2 when subjected to sand and water

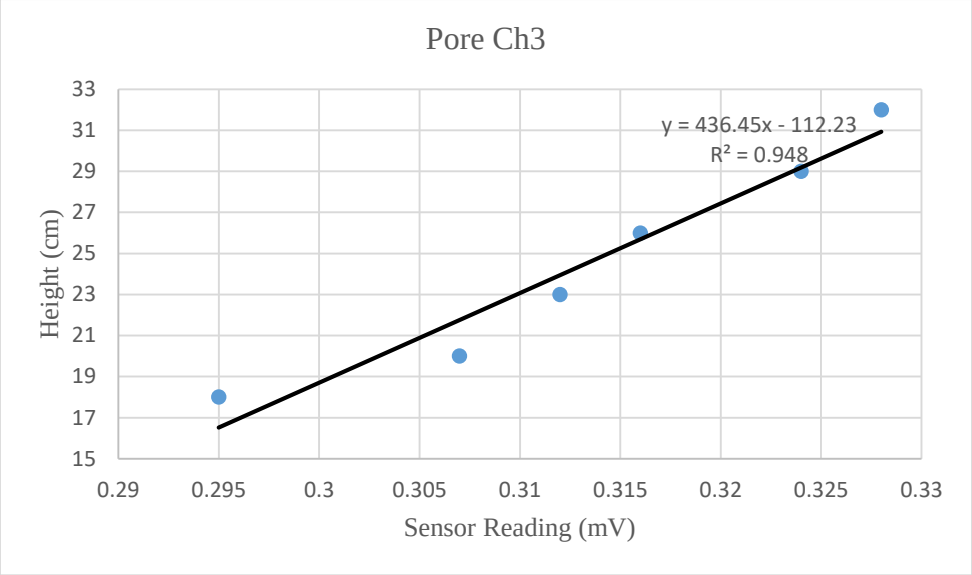

Figure 3-16: Graph for water sensor 3 when subjected to sand and water

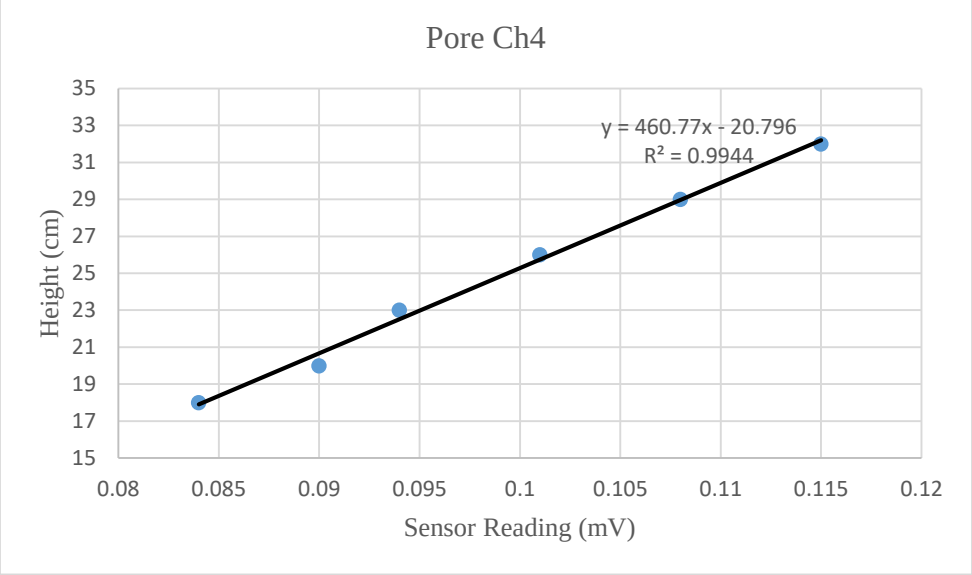

Figure 3-17: Graph for water sensor 4 when subjected to sand and water

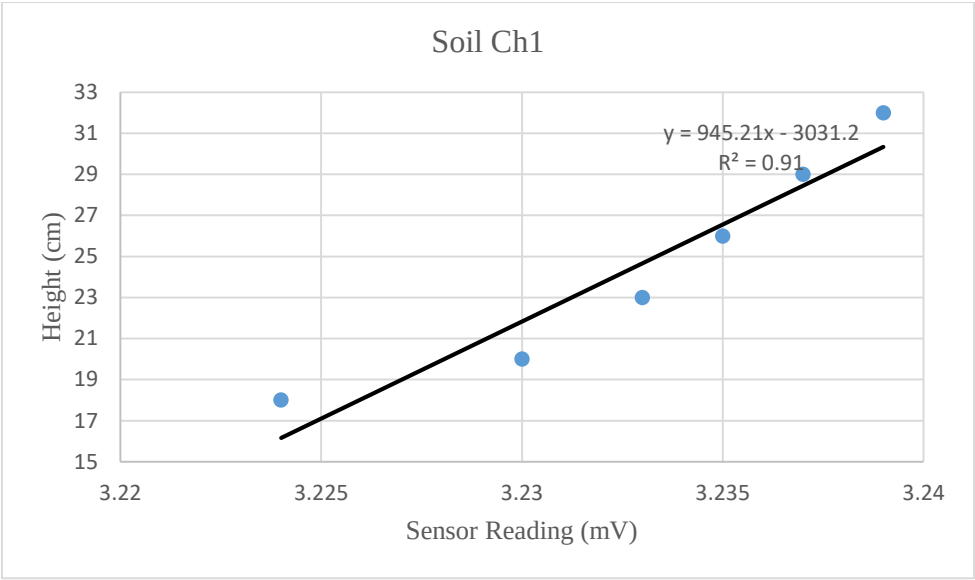

Figure 3-18: Graph for soil sensor 1 when subjected to sand and water

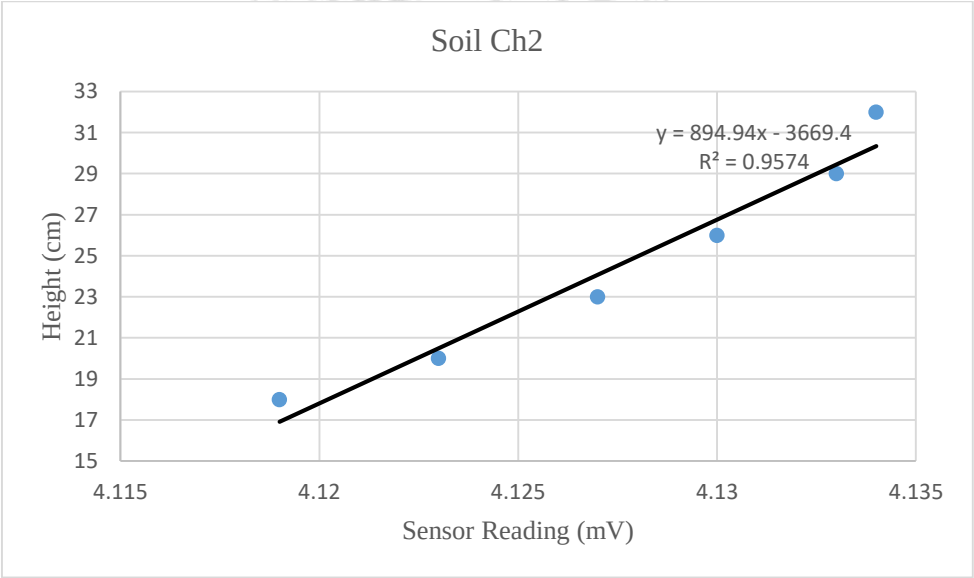

Figure 3-19: Graph for soil sensor 2 when subjected to sand and water

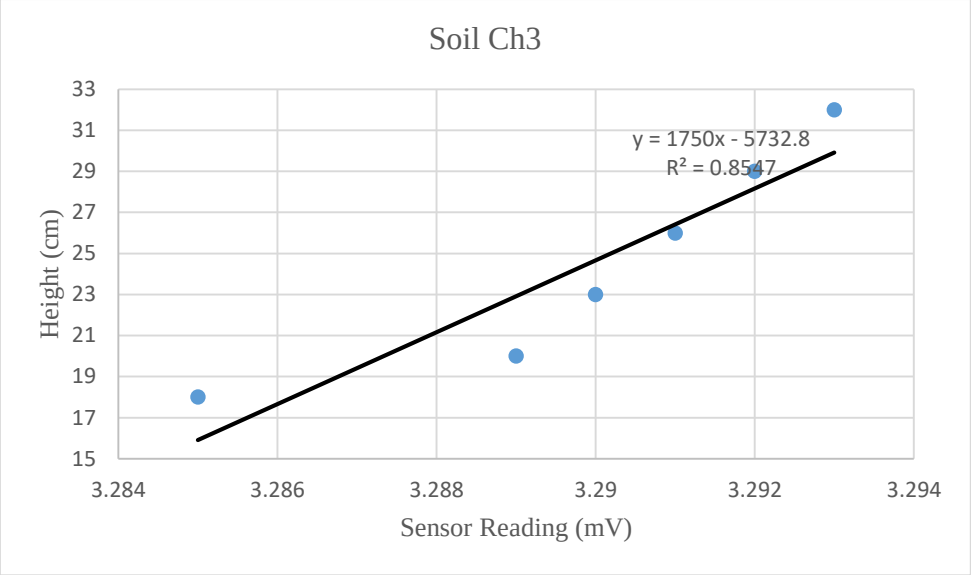

Figure 3-20: Graph for soil sensor 3 when subjected to sand and water

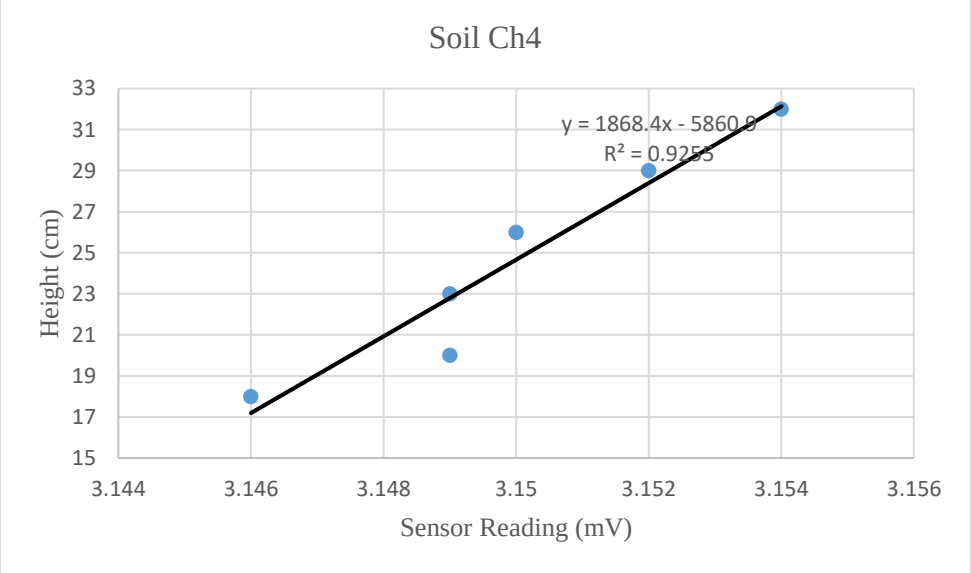

Figure 3-21: Graph for soil sensor 4 when subjected to sand and water

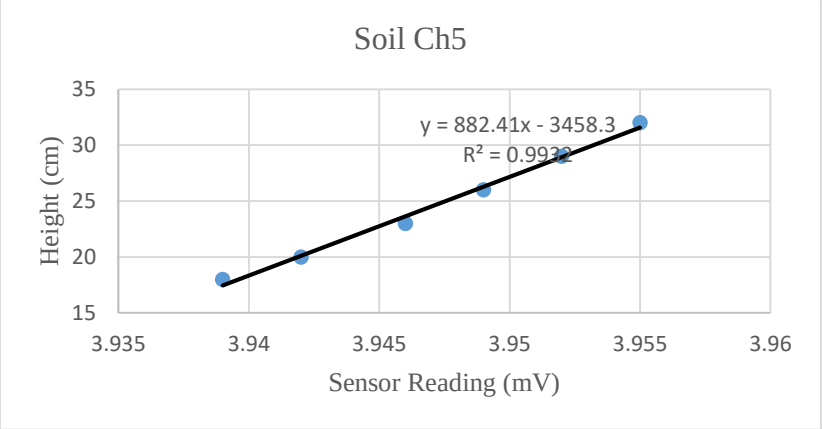

Figure 3-22: Graph for soil sensor 5 when subjected to sand and water

3.2.2. Sandbox Experiment

Sandbox experiment is an equation where a prototype of the landslide dam is made in a box and exposed to water pressure. To recreate a similar environment as the actual case of the field.

Procedure

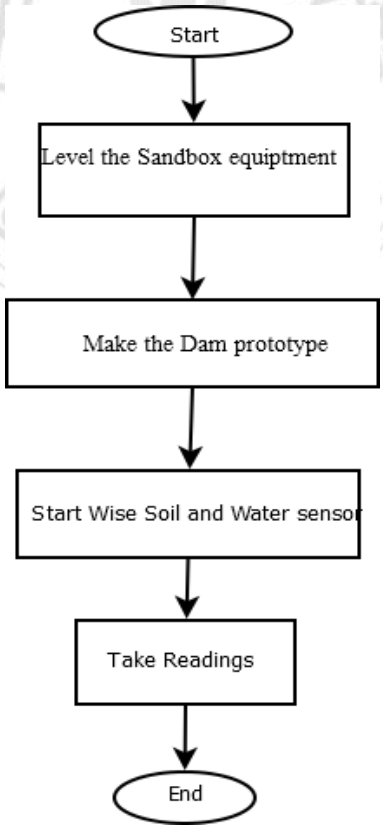

Experiment setup:

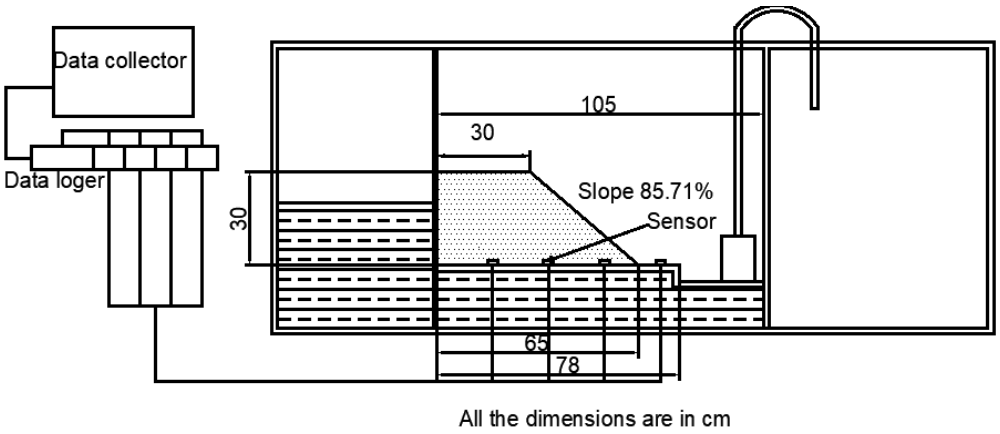

Figure 3-23: Schemetic diadram of Experimental sutup

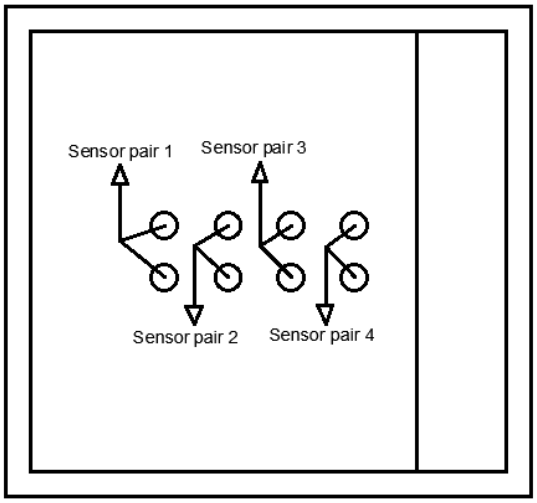

Figure 3-24: Layout of sensor placement

Figure 3-25: Experimental Setup

Dimensions

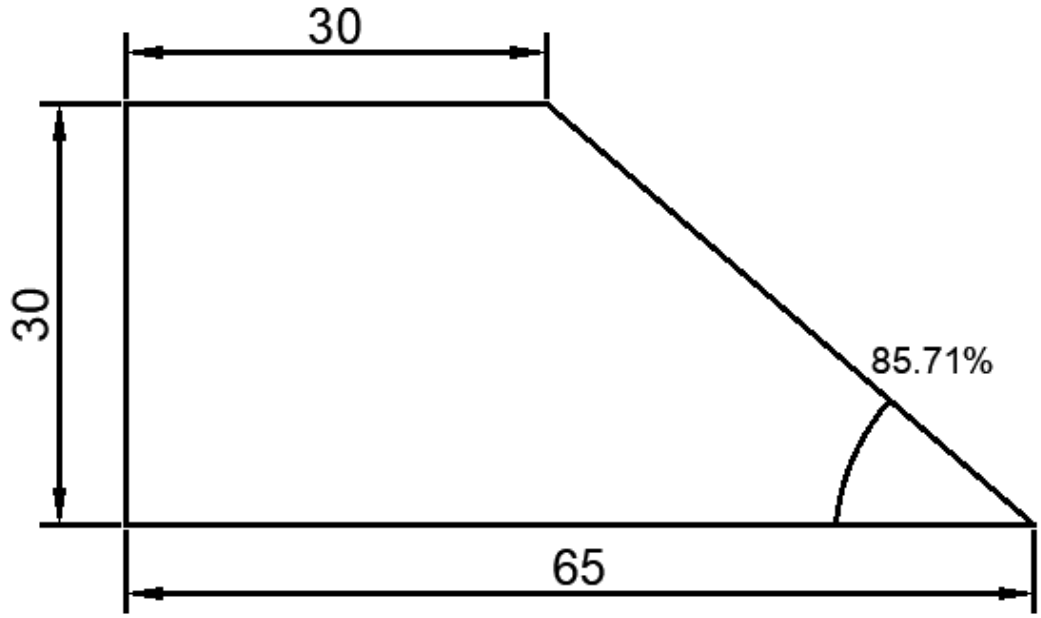

Figure 3-26: Landslide Dam prototype Dimensions

1. Height of the dam: 30cm
2. Slope angle: 85.71%
3. Base length: 65cm
4. Top length: 30cm

The diagram in Figure 3 26 shows the experimental setup of the sandbox experiment. The trapezoidal shape in the middle of the sandbox equipment is the landslide dam prototype. The height of the dam is 30 cm and the length is 65 cm. The slope is kept at 85.71%. The angle of the slope is 40.600.

Chapter 4: Result and Discussion

4.1. Result

The following figures shows the outcome of the sandbox experiment. The sensor pairs 1, 2, 3 were under the dam prototype from the start, but sensor pair 4 was outside the dam prototype. That pair of sensors came under the contact of any water or sand was after the dam has started to breach. The experiment is done three times with different groundwater levels 16cm, 18cm, 20cm respectively. The results from the experiments are discussed bellow.

Figure 4-1: Setup for groundwater level 16cm

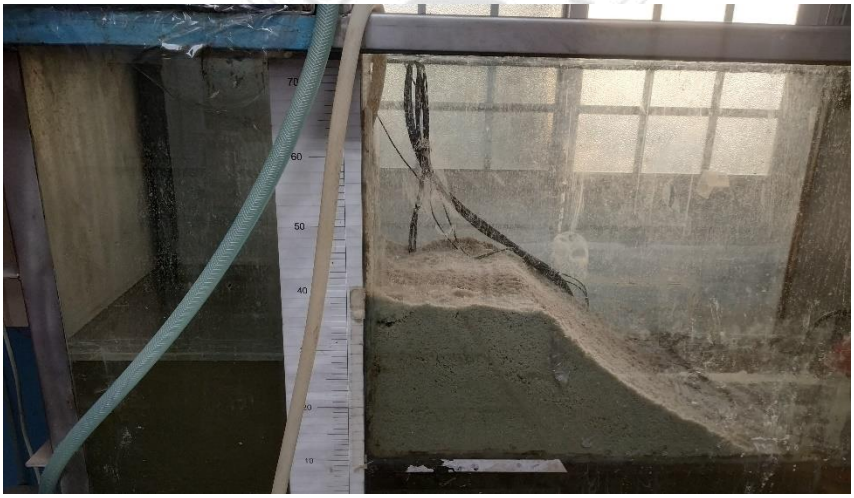

Figure 4-2: Setup for groundwater level 18cm

Figure 4-3: Setup for groundwater level 18cm

Figure 4-4: Did not fail only seepage and crack ground water 16cm.

(a) Top view (b) Side view

Figure 4-5: Failure of dam

(b) Top view (b) Side view

Figure 4-6: After the failure of the dam at groundwater 20cm

Groundwater 16cm

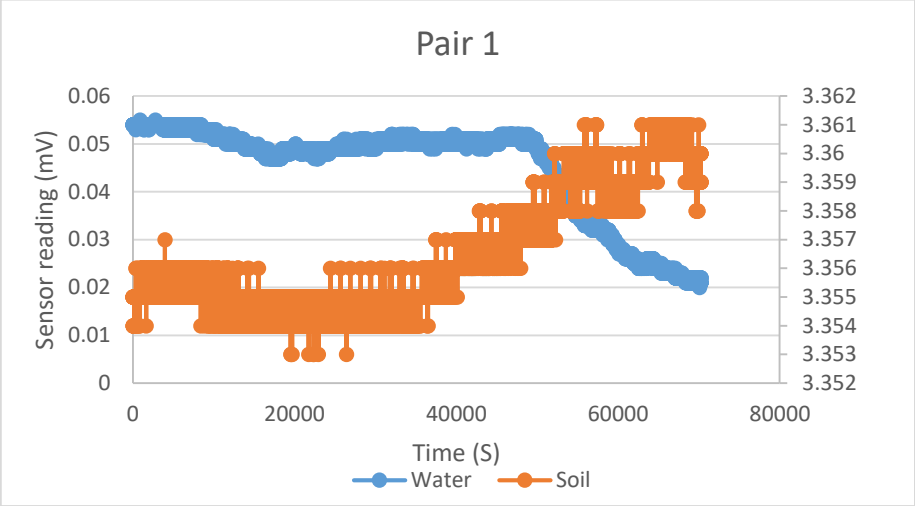

Figure 4-7: Sensor Reading Pair 1 groundwater 16cm

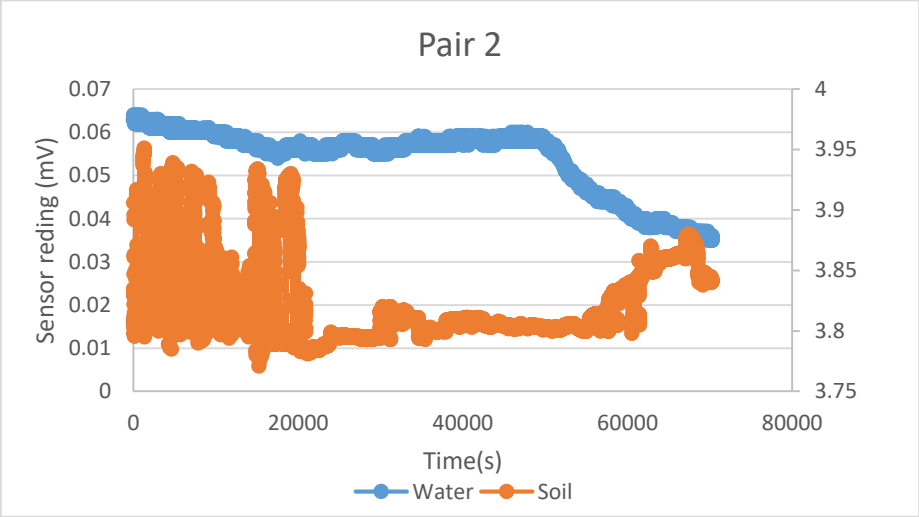

Figure 4-8: Sensor Reading Pair 2 groundwater 16cm

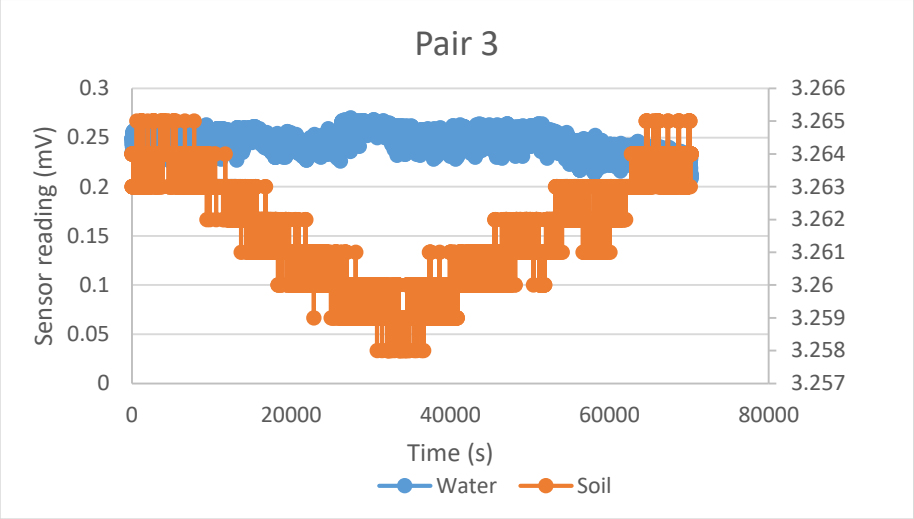

Figure 4-9: Sensor Reading Pair 3 groundwater 16cm

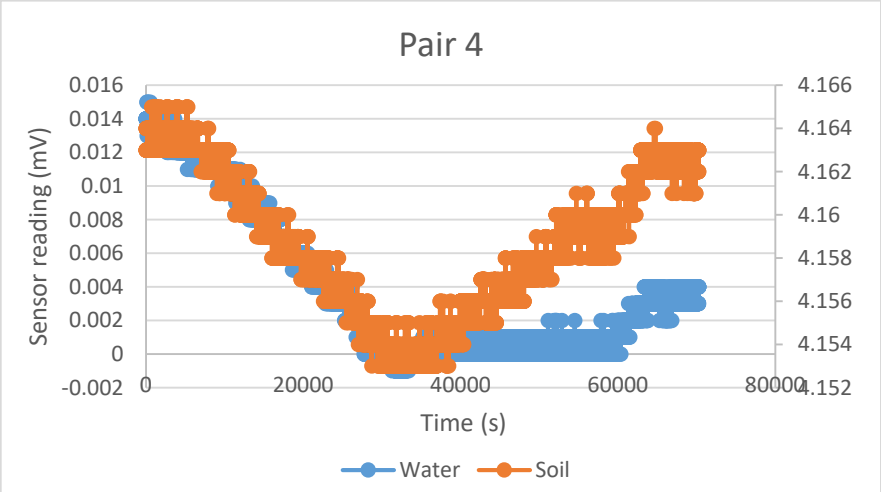

Figure 4-10: Sensor Reading Pair 4 groundwater 16cm

The dam did not fail when the groundwater level was at 16cm. Therefore, there is no drop in soil pressure. The drop in water level is because of the seepage flow as the water flowed out.

Groundwater 18cm

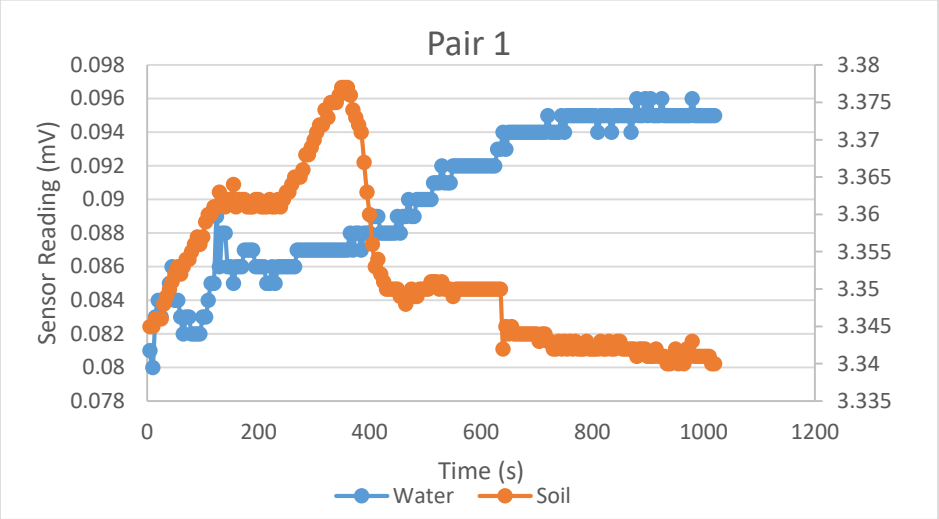

Figure 4-11: Sensor Reading Pair 1 groundwater 18cm

The above Figure 4-11 the characteristics of sand and water pressure on sensor pair 1. In this, it can be observed that the sand pressure dropped after the 600-second mark. That is the time when the dam failed. The 400-second mark to the 600-second mark is the period of breaching of sand in the dam. That is because of the bulking of sand as its density decreases due to an increase in water level. As for the water pressure, it has an average increment after the 200-second mark till the end. The water reached sensor pair 1 at the 200-second mark.

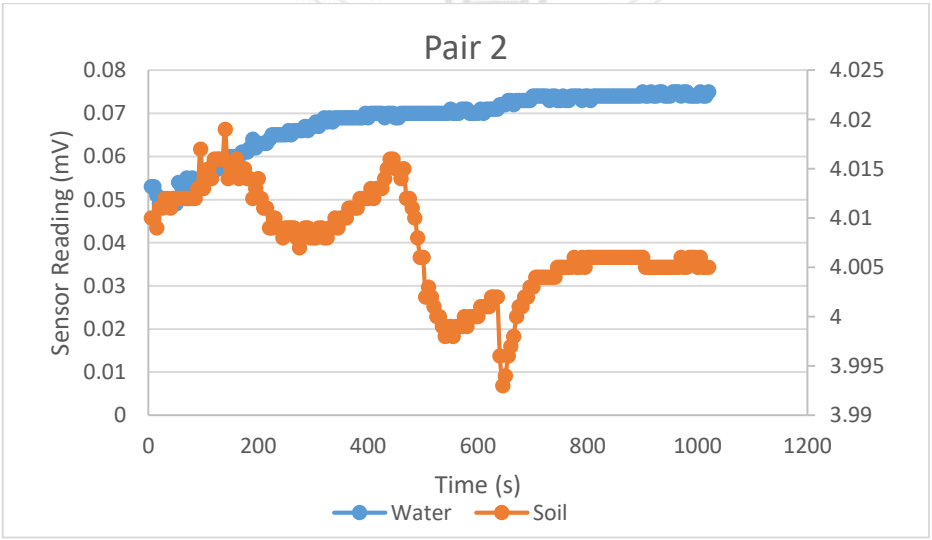

Figure 4-12: Sensor Reading Pair 2 groundwater 18cm

The above Figure 4-12 is the characteristics of sand and water pressure on sensor pair 2. In this, it can be observed that the sand pressure dropped after the 600-second mark. That is the time when the dam failed. The 400-second mark to the 600-second mark is the period of breaching of sand in the dam. That is because of the bulking of sand as its density decreases due to an increase in water level. As for the water pressure, it has an average increment after the 200-second mark till the end. The water reached sensor pair 2 at the 200-second mark.

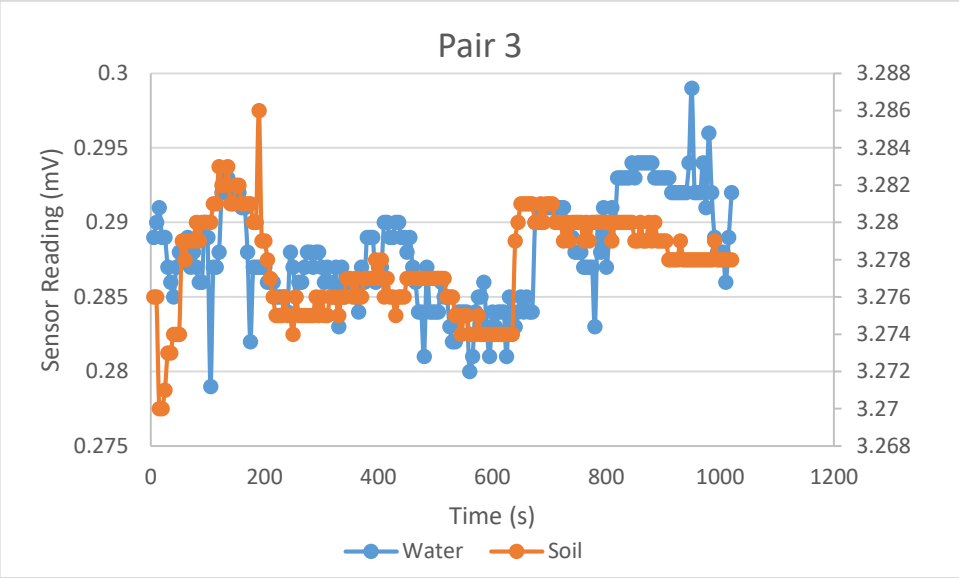

Figure 4-13: Sensor Reading Pair 3 groundwater 18cm

The above Figure 4-13 is the characteristics of sand and water pressure on sensor pair 3. In this, it can be observed that the sand pressure sharply raised after the 600-second mark. As for the water pressure, I has increased sharply a bit after the soil pressure rise.

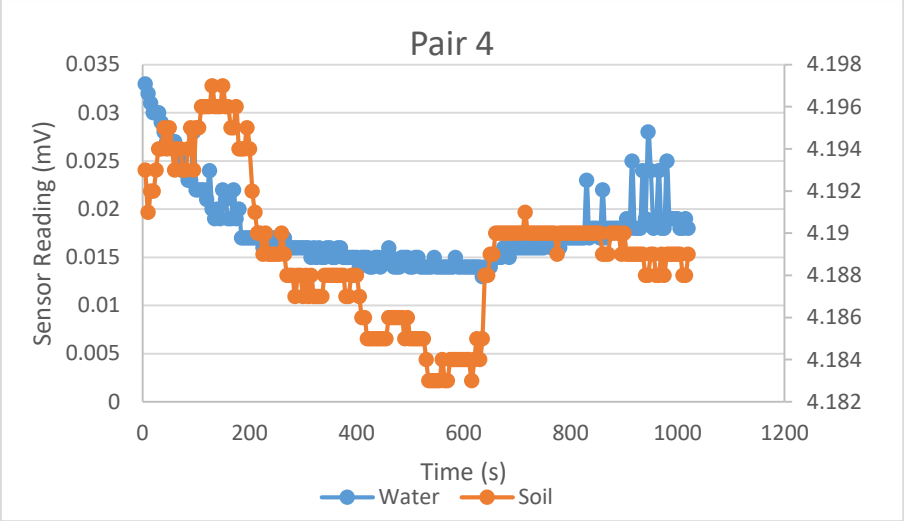

Figure 4-14: Sensor Reading Pair 4 groundwater 18cm

The above Figure 4-14 The above figure is the characteristics of sand and water pressure on sensor pair 4. In this, it can be observed that the sand pressure sharply raised after the 600-second mark. As for the water pressure, it hasn't changed a lot.

Groundwater 20cm

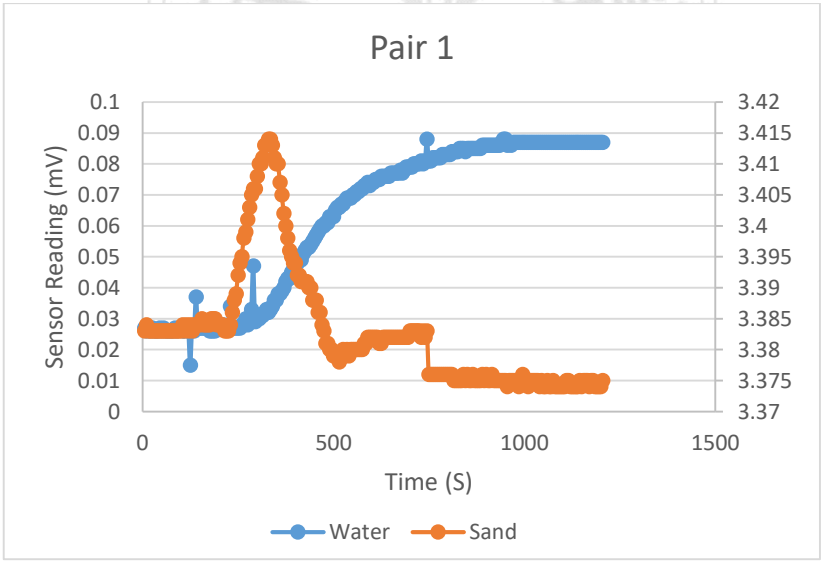

Figure 4-15: Sensor Reading Pair 1 groundwater 20cm

The above Figure 4-15 is the characteristics of sand and water pressure on sensor pair 1. In this, it can be observed that the sand pressure dropped after the 650-second mark. That is the time when the dam failed. The 450-second mark to the 650-second mark is the period of breaching of sand in the dam. That is because of the bulking of sand as its density decreases due to an increase in water level. As for the water pressure, it has an average increment

after the 250-second mark till the end. The water reached sensor pair 1 at the 250-second mark.

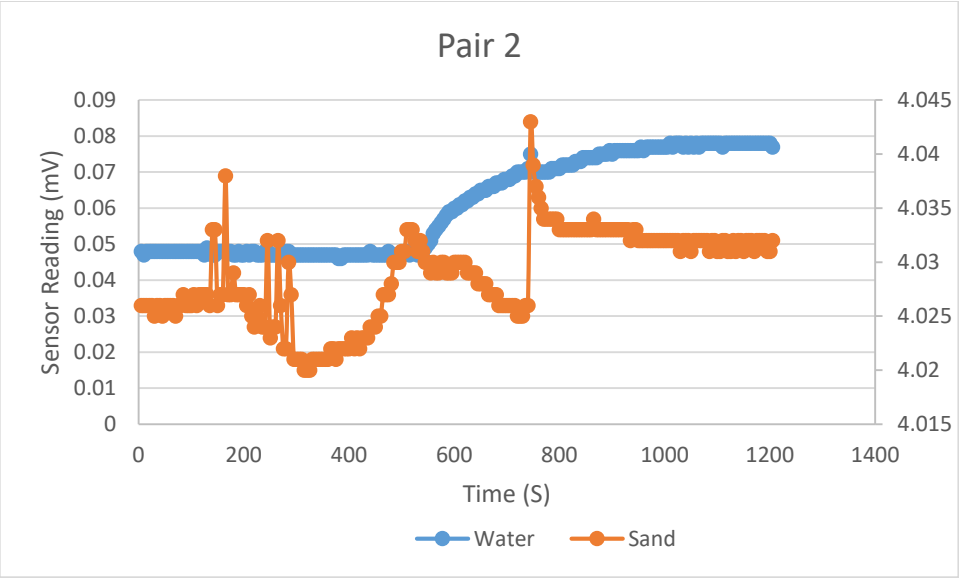

Figure 4-16: Sensor Reading Pair 2 groundwater 20cm

The above Figure 4-16 is the characteristics of sand and water pressure on sensor pair 2. In this, it can be observed that the sand pressure sharply increaded after the 680-second mark. That is the time when the dam failed. The 450-second mark to the 680-second mark is the period of breaching of sand in the dam. That is because of the bulking of sand as its density decreases due to an increase in water level. As for the water pressure, it has an average increment after the 450-second mark till the end. The water reached sensor pair 2 at the 450-second mark.

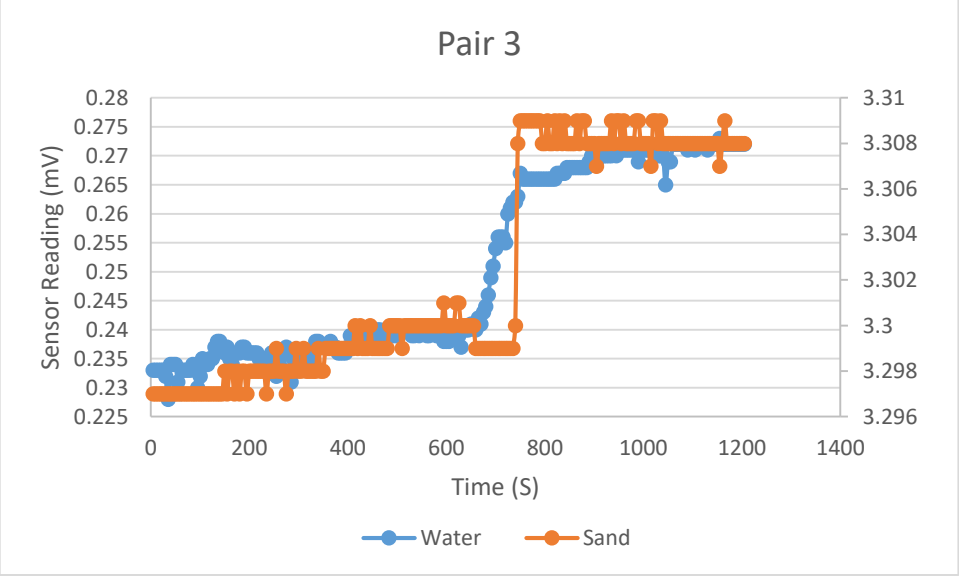

Figure 4-17: Sensor Reading Pair 3 groundwater 20cm

The above Figure 4-17 is the characteristics of sand and water pressure on sensor pair 3. In this, it can be observed that the sand pressure sharply increased after the 680-second mark. That is the time when the dam failed. The 450-second mark to the 680-second mark is the period of breaching of sand in the dam. That is because of the bulking of sand as its density decreases due to an increase in water level. As for the water pressure, it has an sharp increment after the 600-second mark till the end. The water reached sensor pair 3 at the 600-second mark.

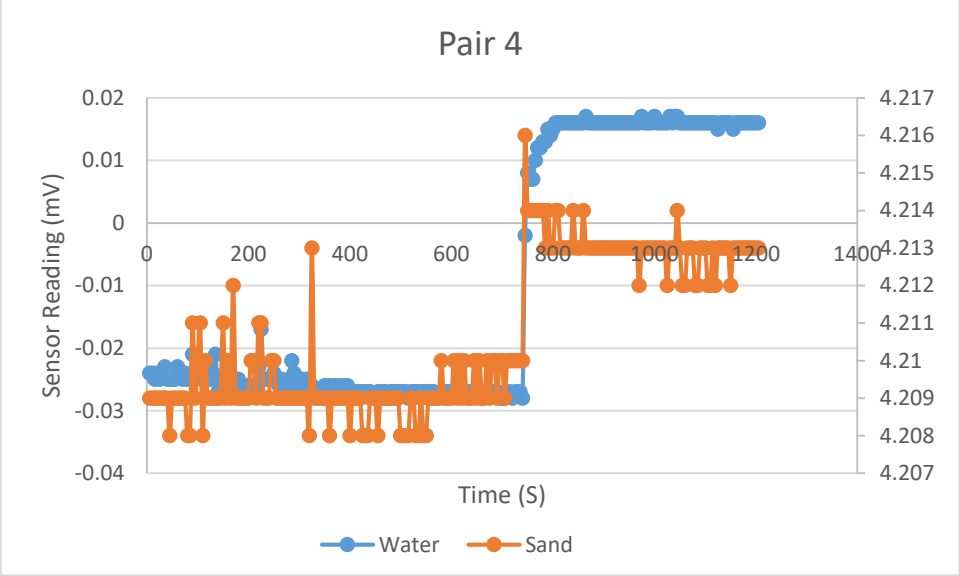

Figure 4-18: Sensor Reading Pair 4 groundwater 20cm

The above Figure 4-18 is the characteristics of sand and water pressure on sensor pair 4. In this, it can be observed that the sand pressure sharply increased after the 680-second mark. That is the time when the dam failed. The 450-second mark to the 680-second mark is the period of breaching of sand in the dam. That is because of the bulking of sand as its density decreases due to an increase in water level. As for the water pressure, it has a sharp increment after the 600-second mark till the end. The water reached sensor pair 4 at the 600-second mark.

4.2. Discussion

The sandbox experiment conducted shows the laboratory level demonstration of the failure of the landslide dam. From the outcome of the experiment it is found that the dam failed when it is subjected to a groundwater of height 18cm or more. Therefore the critical ground water level for the dam failure is 18cm.

The relation between the failure of the dam and the water level developed before (equation 6) can be implemented here to match with the outcome of the experiment and the prediction value. From the governing equation putting all the parameters the critical level of water can be determined.

$$H_{wc} = (\gamma/\gamma_w)\mathrm{H} - (\gamma H \sin\alpha \cos\alpha - c)/(\gamma_w \cos^2\alpha \tan\varphi) \qquad (6)$$

c'=1.019 kPa = 10.39 g/cm^2

φ'=0.64228 rad

α=0.7086 rad

γ=1.432g/cc

γ_w=1g/cc

H=23.5 cm

Putting all these values in eq (6):

H_w= 19.177 cm

According to the experiment the critical ground water level for the dam to fail is 18cm. According to the governing equation the critical ground water level is 19.177 cm. There is a mismatch of 6.54% between experimental result and the result from the governing equation.

Chapter 5: Conclusion

5.1. Conclusion

In this study, an experimental approach has been adopted to justify a governing equation for determining the critical water level for the failure of a landslide dam. The governing equation was established by considering the infinite slope method. The stability analysis was done under a critical condition when the resisting force equals the destabilizing force. A small prototype landslide dam is recreated in the laboratory to perform the sandbox experiment. The slope angle is kept at 85.71%. In this experiment the dam prototype started failing due to the seepage erosion in the sample prototype. The sandbox experiment has been done in different level of ground water. The governing equation gave a critical value of 19.117cm for the failure of the landslide dam due to seepage erosion. The experiment was done wile keeping the ground water level at 16cm, 18cm, and 20cm. In the experimental result it has been found that the dam prototype failed when the groundwater level was at 18cm. In the experiment it was observed that at first the water seepage starts to occur in the soil, which loosens the friction in the soil particles. This leads the soil mass to slide above a certain height. The water level in the experiment totally justifies the water level from the governing equation developed in this study. Therefore the governing equation can be used to predict the water level for the failure of the landslide dam. Which can be helpful for developing a warning system from the upcoming flood in the downstream by the failure of the landslide dam.

Moreover, further study should be done in this topic by altering the soil composition and slope angles to observe the equation's reliability. The results may be different in different soil profile and different slope angles. This study was done in a controlled environment in the laboratory. So, this experiment can be done in open environment to recreate the similar situation of a landslide

dam. The governing equation used in this study is based on the infinite slope stabilization method. Other slope stabilization method can be used to develop the governing equation also which may lead to more accurate results for the critical ground water level prediction.

References

1. Ahmad, M. A. (n.d.). *Effect of Groundwater Level toward Slope Stability*. 41.

2. Awal, R., Nakagawa, H., Baba, Y., & Sharma, R. H. (2007). NUMERICAL AND EXPERIMENTAL STUDY ON LANDSLIDE DAM FAILURE BY SLIDING. *PROCEEDINGS OF HYDRAULIC ENGINEERING, 51*, 7–12. https://doi.org/10.2208/prohe.51.7

3. Beach, T., Dunning, N., Luzzadder-Beach, S., Cook, D. E., & Lohse, J. (2006). Impacts of the ancient Maya on soils and soil erosion in the central Maya Lowlands. *CATENA*, *65*(2), 166–178. https://doi.org/10.1016/j.catena.2005.11.007

4. Becker, J. S., Johnston, D. M., Paton, D., Hancox, G. T., Davies, T. R., McSaveney, M. J., & Manville, V. R. (2007). Response to Landslide Dam Failure Emergencies: Issues Resulting from the October 1999 Mount Adams Landslide and Dam-Break Flood in the Poerua River, Westland, New Zealand. *Natural Hazards Review*, *8*(2), 35–42. https://doi.org/10.1061/(ASCE)1527-6988(2007)8:2(35)

5. Budhu, M., & Gobin, R. (1995). Seepage Erosion from Dam-Regulated Flow: Case of Glen Canyon Dam, Arizona. *Journal of Irrigation and Drainage Engineering*, *121*(1), 22–33. https://doi.org/10.1061/(ASCE)0733-9437(1995)121:1(22)

6. Cao, Z., Yue, Z., & Pender, G. (2011). Landslide dam failure and flood hydraulics. Part I: Experimental investigation. *Natural Hazards*, *59*(2), 1003–1019. https://doi.org/10.1007/s11069-011-9814-8

7. Collins, B. D., & Znidarcic, D. (2004). Stability analyses of rainfall induced landslides. *Journal of Geotechnical and Geoenvironmental Engineering*, *130*(4), 362–372.

8. Corominas, J., Moya, J., Ledesma, A., Lloret, A., & Gili, J. A. (2005). Prediction of ground displacements and velocities from groundwater level changes at the Vallcebre landslide (Eastern Pyrenees, Spain). *Landslides*, *2*(2), 83–96. https://doi.org/10.1007/s10346-005-0049-1

9. Costa, J. E., & Schuster, R. L. (1988). The formation and failure of natural dams. *GSA Bulletin*, *100*(7), 1054–1068. https://doi.org/10.1130/0016-7606(1988)100<1054:TFAFON>2.3.CO;2

10. Davies, T. R. H., & Korup, O. (2007). Persistent alluvial fanhead trenching resulting from large, infrequent sediment inputs. *Earth Surface Processes and Landforms*, *32*(5), 725–742. https://doi.org/10.1002/esp.1410

11. Dunning, S. A., Rosser, N. J., Petley, D. N., & Massey, C. R. (2006). Formation and failure of the Tsatichhu landslide dam, Bhutan. *Landslides*, *3*(2), 107–113. https://doi.org/10.1007/s10346-005-0032-x

12. Eisbacher, G. H. (1984). *Destructive mass movements in high mountains*. Geological Survey of Canada.

13. Ergenzinger, P. (n.d.). *A conceptual geomorphological model for the development of a Mediterranean river basin under neotectonic stress (Buonamico basin, Calabria, Italy)*. 10.

14. Evans, S. G. (1986). *Landslide Damming in the Cordillera of Western Canada*. 111–130. https://cedb.asce.org/CEDBsearch/record.jsp?dockey=0048096

15. Evans, S. G., Delaney, K. B., Hermanns, R. L., Strom, A., & Scarascia-Mugnozza, G. (2011). The Formation and Behaviour of Natural and Artificial Rockslide Dams; Implications for Engineering Performance and Hazard Management. In S. G. Evans, R. L. Hermanns, A. Strom, & G. Scarascia-Mugnozza (Eds.), *Natural and Artificial Rockslide Dams* (pp. 1–75). Springer. https://doi.org/10.1007/978-3-642-04764-0_1

16. Ghiassian, H., & Ghareh, S. (2008). Stability of sandy slopes under seepage conditions. *Landslides*, *5*(4), 397–406. https://doi.org/10.1007/s10346-008-0132-5

17. Glazyrin, G. Y., & Reyzvikh, V. N. (1968). Computation of the flow hydrograph for the breach of landslide lakes. *Soviet Hydrology*, *5*, 492–496.

18. Guerricchio, A. (1973). *SEGNI PREMONITORI E COLLASSI DELLE GRANDI FRANE NELLE METAMORFITI DELLA VALLE DELLA FLUMARA BUONAMICO (ASPROMONTE, CALABRIA).*

19. Gündo, B. (n.d.). *MIDDLE EAST TECHNICAL UNIVERSITY*. 115.

20. Hancox, G. T., McSaveney, M. J., Manville, V. R., & Davies, T. R. (2005). The October 1999 Mt Adams rock avalanche and subsequent landslide dam-break flood and effects in Poerua river, Westland, New Zealand. *New Zealand Journal of Geology and Geophysics*, *48*(4), 683–705. https://doi.org/10.1080/00288306.2005.9515141

21. Hermanns, R. L. (2013). Landslide Dam. In P. T. Bobrowsky (Ed.), *Encyclopedia of Natural Hazards* (pp. 602–606). Springer Netherlands. https://doi.org/10.1007/978-1-4020-4399-4_213

22. Hermanns, R. L., Niedermann, S., Ivy-Ochs, S., & Kubik, P. W. (2004). Rock avalanching into a landslide-dammed lake causing multiple dam failure in Las Conchas valley (NW Argentina)—Evidence from surface exposure dating and stratigraphic analyses. *Landslides*, *1*(2), 113–122. https://doi.org/10.1007/s10346-004-0013-5

23. Holland, T. H. (1894). Report on the Gohna landslip, Garhwal. *Records Geol. Surv. of India*, *27*, 55–65.

24. Jiang, X., Zhanyuan, Z., Chen, H., Deng, M., Niu, Z., Deng, H., & Zuyin, Z. (2020). Natural dam failure in slope failure mode triggered by seepage. *Geomatics, Natural Hazards and Risk*, *11*(1), 698–723. https://doi.org/10.1080/19475705.2020.1746697

25. King, J., Loveday, I., & Schuster, R. L. (1989). The 1985 Bairaman landslide dam and resulting debris flow, Papua New Guinea. *Quarterly*

Journal of Engineering Geology and Hydrogeology, *22*(4), 257–270. https://doi.org/10.1144/GSL.QJEG.1989.022.04.02

26. Korup, O. (2002). Recent research on landslide dams-a literature review with special attention to New Zealand. *Progress in Physical Geography*, *26*(2), 206–235.

27. McColl, S. T. (2015). Chapter 2—Landslide Causes and Triggers. In J. F. Shroder & T. Davies (Eds.), *Landslide Hazards, Risks and Disasters* (pp. 17–42). Academic Press. https://doi.org/10.1016/B978-0-12-396452-6.00002-1

28. Meyer, W., Schuster, R. L., & Sabol, M. A. (1994). Potential for Seepage Erosion of Landslide Dam. *Journal of Geotechnical Engineering*, *120*(7), 1211–1229. https://doi.org/10.1061/(ASCE)0733-9410(1994)120:7(1211)

29. Montandon, F. (1933). *Chronologie des grands éboulements alpins: Du début de l'ère chrétienne à nos jours*.

30. Pushkarenko, V. P., & Nikitin, A. M. (1988). Experience in the regional investigation of the state of mountain lake dams in central Asia and the character of breach mudflow formation. *Landslides and Mudflows. UNEP/UNESCO, Moscow*, 359–362.

31. Regmi, R. K., Lee, G., & Jung, K. (2013). Analysis on failure of slope and landslide dam. *KSCE Journal of Civil Engineering*, *17*(5), 1166–1178. https://doi.org/10.1007/s12205-013-0049-y

32. SCHUSTER, R. L. (2006). IMPACTS OF LANDSLIDE DAMS ON MOUNTAIN VALLEY MORPHOLOGY. In S. G. Evans, G. S. Mugnozza, A. Strom, & R. L. Hermanns (Eds.), *Landslides from Massive Rock Slope Failure* (pp. 591–616). Springer Netherlands. https://doi.org/10.1007/978-1-4020-4037-5_31

33. Snow, D. T. (1964). Landslide of Cerro Condor-Sencca, Department of Ayacucho, Peru. *Engineering Geology Case Histories. Geological Society of America*, *5*, 1–6.

34. Sorriso-Valvo, M., Gullà, G., Antronico, L., Tansi, C., & Amelio, M. (1999). Mass-movement, geologic structure and morphologic evolution of the Pizzotto–Greci slope (Calabria, Italy). *Geomorphology*, *30*(1), 147–163. https://doi.org/10.1016/S0169-555X(99)00051-3

35. Terzaghi, K. (1962). Stability of steep slopes on hard unweathered rock. *Geotechnique*, *12*(4), 251–270.

36. Vandamme, J., & Zou, Q. (2013). Investigation of slope instability induced by seepage and erosion by a particle method. *Computers and Geotechnics*, *48*, 9–20. https://doi.org/10.1016/j.compgeo.2012.09.009

37. Walder, J. S., & O'Connor, J. E. (1997). Methods for predicting peak discharge of floods caused by failure of natural and constructed earthen dams. *Water Resources Research*, *33*(10), 2337–2348. https://doi.org/10.1029/97WR01616

38. Wang, F., Dai, Z., Okeke, C. A. U., Mitani, Y., & Yang, H. (2018). Experimental study to identify premonitory factors of landslide dam failures. *Engineering Geology*, *232*, 123–134. https://doi.org/10.1016/j.enggeo.2017.11.020

39. Zhu, X., Peng, J., Liu, B., Jiang, C., & Guo, J. (2020). Influence of textural properties on the failure mode and process of landslide dams. *Engineering Geology*, *271*, 105613. https://doi.org/10.1016/j.enggeo.2020.105613

40. 洪耀明（2019），整合地文與水文資訊之深層崩塌即時預警模式(I)，行政院農業委員會水土保持局。